A Neuro-Sliding-Mode Control With Adaptive Modeling of Uncertainty for Control of Movement in Paralyzed Limbs Using Functional Electrical Stimulation

Arash Ajoudani and Abbas Erfanian*, *Member, IEEE*

***Abstract*—During the past several years, several strategies have been proposed for control of joint movement in paraplegic subjects using functional electrical stimulation (FES), but developing a control strategy that provides satisfactory tracking performance, to be robust against time-varying properties of muscle–joint dynamics, day-to-day variations, subject-to-subject variations, muscle fatigue, and external disturbances, and to be easy to apply without any re-identification of plant dynamics during different experiment sessions is still an open problem. In this paper, we propose a novel control methodology that is based on synergistic combination of neural networks with sliding-mode control (SMC) for controlling FES. The main advantage of SMC derives from the property of robustness to system uncertainties and external disturbances. However, the main drawback of the standard sliding modes is mostly related to the so-called chattering caused by the high-frequency control switching. To eliminate the chattering, we couple two neural networks with online learning without any offline training into the SMC. A recurrent neural network is used to model the uncertainties and provide an auxiliary equivalent control to keep the uncertainties to low values, and consequently, to use an SMC with lower switching gain. The second neural network consists of a single neuron and is used as an auxiliary controller. The control law will be switched from the SMC to neural control, when the state trajectory of system enters in some boundary layer around the sliding surface. Extensive simulations and experiments on healthy and paraplegic subjects are provided to demonstrate the robustness, stability, and tracking accuracy of the proposed neuroadaptive SMC. The results show that the neuro-SMC provides accurate tracking control with fast convergence for different reference trajectories and could generate control signals to compensate the muscle fatigue and reject the external disturbance.**

***Index Terms*—Functional electrical stimulation (FES), neural network, sliding-mode control (SMC).**

I. Introduction

FUNCTIONAL neuromuscular stimulation (FNS) is a promising technique for restoring movement to paralyzed limbs following spinal cord injury, head injury, stroke, and multiple sclerosis [1]–[5]. In FNS systems, sequences of current pulses excite the intact peripheral axon, which, in turn, contract paralyzed muscles. By changing the pulse width, pulse amplitude, or the pulse frequency, the level of contraction can be altered to perform a specific task. To provide functional use of the paralyzed limbs, an appropriate electrical stimulation pattern should be delivered to a set of muscles.

A major impediment to stimulating the paralyzed neuromuscular systems and determining the stimulation pattern has been the highly nonlinear, time-varying properties of electrically stimulated muscle, muscle fatigue, spasticity, and day-to-day variations that limit the utility of prespecified stimulation pattern and open-loop FNS control system. To deal with these problems, many control strategies have been developed, tested, and reported in the literature, including fixed-parameter feedback controller [6], [7], adaptive feedback techniques [8]–[11], fixed-parameter feedforward [12], [13], and adaptive feedforward [13]–[18]. Moreover, in some studies, the combination of feedforward and feedback control techniques have been proposed [12], [13], [19] to utilize the advantages of both controller. In particular, Chang *et al.* [12] used a time-invariant multilayered feedforward neural network to model the inverse of the muscle–joint dynamics for direct feedforward control. To compensate for the residual tracking errors, a fixed-parameter proportional integral derivative (PID) feedback controller was also added that was designated as a neuro-PID controller. The results on one able-bodied and one paraplegic subject showed that the tracking performance of the neuro-PID is slightly better than that of PID controller alone and neural feedforward controller alone. The same result was reported by Kurosawa *et al.* [19] while an adaptive neural network was used as the feedforward controller and a PID as the feedback component for controlling the palmar/dorsi-flexion angle of the wrist.

Ferrarin *et al.* [13] employed four different control strategies including fix-parameter feedforward, fix-parameter feedback using PID, combination of fixed-parameter feedback (e.g., PID) and feedforward, and an adaptive feedforward controller to control the movement of the freely swinging shank. The results of simulations and experiments on two paraplegic subjects showed that the adaptive controller provides a better performance than the other three controllers with fixed parameters. The performance of combined feedback and feedforward controller is better than that of feedback alone and feedforward

Manuscript received February 7, 2008; revised November 6, 2008. First published March 27, 2009; current version published June 12, 2009. This work was supported by the Iran University of Science and Technology (IUST). *Asterisk indicates corresponding author.*

A. Ajoudani is with the Department of Biomedical Engineering, Iran University of Science and Technology (IUST), Tehran 16846-13114, Iran.

*A. Erfanian is with the Department of Biomedical Engineering, Faculty of Electrical Engineering, Iran Neural Technology Research Center, Iran University of Science and Technology (IUST), Tehran 16846-13114, Iran (e-mail: erfanian@iust.ac.ir).

Color versions of one or more of the figures in this paper are available online at http://ieeexplore.ieee.org.

Digital Object Identifier 10.1109/TBME.2009.2017030

alone. This result is in accordance with the work of Chang *et al.* [12].

All the earlier mentioned works indicate that the tracking quality was improved by the use of the adaptive control law compared to the nonadaptive one. Adaptive control, by online tuning the parameters (of either the plant or the controller—corresponding to indirect or direct adaptive control), can deal with uncertainties, but generally suffers from the disadvantage of being able to achieve only *asymptotical* convergence of the tracking error to zero. Generally, this algorithm is based on the assumption that the structure of the system model is known with unknown system slow-varying parameters and the parameters appear linear. Several issues, such as transient performance, unmodeled dynamics, disturbance, the amount of offline training required, the tradeoff between the persistent excitation of signals for correct identification and the steady system response for control performance, the model convergence and system stability issues in real applications, and nonlinearity in parameters, often complicate the adaptive approach [20]–[23].

A useful and powerful robust control scheme to deal with the uncertainties, nonlinearities, and bounded external disturbances is the sliding-mode control (SMC) [24]. These uncertainties may come from unmodeled dynamics, variations in system parameters, or approximations of complex plant behaviors. In robust control designs, a fixed control law based on *a priori* information on the uncertainties is designed to compensate for their effects, and *exponential* convergence of the tracking error to a (small) ball centered at the origin is obtained. Robust control has some advantages over the adaptive control, such as its ability to deal with disturbances, quickly varying parameters, and unmodeled dynamics [24]. Nevertheless, the SMC suffers from the high-frequency oscillations in the control input, which is called "chattering" [25].

In order to limit the chattering phenomena and preserve the main advantages of the original SMC, we propose a new SMC by combining adaptive control and neural network with SMC for control of muscle–skeletal systems using functional electrical stimulation in paraplegic subjects. The proposed scheme directly results in chattering free control action for the corrective control. The main motivation for this study is to develop a control scheme for FNS systems that results in stable, repeatable, regulated muscle input-output properties over a wide range of conditions of muscle length, electrode movement, potentiation, fatigue, day-to-day variations, different movement patterns, and different disturbances.

II. Sliding-Mode Control

Consider the following nonlinear system:

$$\ddot{\mathbf{x}} = f(\mathbf{x}, t) + b(\mathbf{x}, t) \cdot u(t) \tag{1}$$

where $f(\mathbf{x}, t)$ and control gain $b(\mathbf{x}, t)$ are unknown nonlinear functions, $x(t)$ is the state variable to be controlled, and $u(t)$ the control input. The objective of the controller is to design a control law to force the system state variable to track the desired state trajectory $x_d(t)$ in the presence of model uncertainties and external disturbances. We first define a sliding surface as follows:

$$s(e, t) = \left(\frac{d}{dt} + \lambda\right)^2 \left(\int_0^t e(r)dr\right) = 0 \tag{2}$$

where e is the state error and λ a positive constant. By solving the equation $\dot{s} = 0$ for the control input using (1), we obtain the following expression for $u(t)$, which is called equivalent control

$$\begin{aligned} u_{\mathrm{eq}}(t) &= \frac{1}{\hat{b}(\mathbf{x}, t)} \cdot \left(-\hat{f}(\mathbf{x}) + \ddot{x}_d(t) - 2\lambda\dot{e}(t) - \lambda^2 e(t)\right) \\ &= \frac{1}{\hat{b}(\mathbf{x}, t)} \cdot \hat{u}(t) \end{aligned} \tag{3}$$

where $\hat{f}$ and $\hat{b}$ are estimations of nonlinear functions f and b, respectively, with the bounded estimation errors. The equivalent control keeps the system states on the sliding surface, once they reach it. Hence, if the states are outside the sliding surface, to drive the states to the sliding surface in finite time, the control law is chosen such that

$$\frac{1}{2}\frac{d}{dt}s^2 \le -\eta\,|s| \tag{4}$$

where η is a strictly positive constant and (4) is called reaching condition [24]. To satisfy the reaching condition, one may choose the following corrective control [24], which is added to the equivalent control

$$u_c = -k \cdot \mathrm{sgn}(s), \qquad k > 0 \tag{5}$$

where $\mathrm{sgn}(s)$denotes the sign of sliding variable. Hence, the whole control input u_1 is a combination of u_{eq} and u_c as

$$u_1(t) = \frac{1}{\hat{b}(\mathbf{x}, t)} \cdot \left[\hat{u}(t) - k \cdot \mathrm{sgn}(s)\right]. \tag{6}$$

This control law leads to high-frequency control switching and chattering across sliding surface. The term "chattering" describes the phenomenon of finite-frequency, finite-amplitude oscillations appearing in many sliding mode implementations. The chattering caused by high-frequency switching control activity is highly undesirable because it leads to low control accuracy and may excite unmodeled high-frequency plant dynamics that could result in unpredictable instability [25]. To overcome this problem, the SMC strategy deserves special attention, because this method provides a systematic approach to maintain asymptotic stability and consistent performance.

A simple method for alleviation of chattering is using a suitable boundary layer around the sliding surface, in which the switching function is approximated by a linear feedback gain when the state trajectory lies within the boundary layer [24]–[26]. Within the boundary layer, the system no longer behaves as dictated by SMC. By introducing boundary layer, chattering can be reduced, but tracking performance and robustness are compromised.

The conventional SMC with boundary layer has been already used for control of knee joint angle in a healthy subject [27]. However, conventional SMC suffers from chattering and poor tracking accuracy. Jezernik *et al.* [28] reported the use of sliding-mode closed-loop controller for the control of knee joint angle. To reduce the chattering, they replaced the discontinuous term,

$k \cdot \mathrm{sgn}(s)$, by a continuous one, $k \cdot s$ in sliding control law. In this case, the finite-time convergence of sliding variable to zero cannot be guaranteed and η-reachability condition will be violated.

III. Methods

One commonly used method to eliminate the effects of chattering is to replace the switching control law by a saturating approximation [24] within a boundary layer around the sliding surface. Inside the boundary layer, the discontinuous switching function is approximated by a continuous function to avoid discontinuity of the control signals. Even though the boundary layer design can alleviate the chattering phenomenon, this approach, however, provides no guarantee of convergence to the sliding mode and involve a tradeoff between chattering and robustness, and results in the existence of the steady-state error.

For solving this drawback, we employed a control methodology that is based on synergistic combination of adaptive control and neural network with SMC. If the system uncertainties are large, the sliding-mode controller would require a high switching gain (5) k with a thicker boundary layer to eliminate the higher chattering effect resulting. However, if we continuously increase the boundary layer thickness, we are actually reducing the feedback system to a system without sliding mode. For smoothness of the control signals, a large boundary layer width is required, but for better control accuracy, a small boundary layer width is preferred. To avoid such a condition, it is necessary to keep switching gain to a small value. The only way to decrease the switching gain k is to decrease the system uncertainty. To decrease the uncertainty, an accurate model of the system is required. For this purpose, we coupled a recurrent neural network (RNN) with online learning into the SMC to model the uncertainties and provide an auxiliary equivalent control for compensating the uncertainties. Moreover, inside the boundary layer, the switching function was replaced by a neural network controller. The control law will be switched from the SMC to neural control, when the state trajectory of system enters in some boundary layer around the sliding surface. The online updating the network parameters is performed in such a way that the output tracking error asymptotically converges to zero.

A. SMC With Adaptive Modeling of Uncertainty

It is well known that the model uncertainty may arise from insufficient information about the system or from the purposeful simplification of mathematical model representation of plant (or unstructured uncertainties) and from inaccuracies on the terms actually included in the model (or structured uncertainties). Accordingly, (1) may be represented by

$$\ddot{\mathbf{x}} = f(\mathbf{x}, t) + \Delta f(\mathbf{x}, t) + b(\mathbf{x}, t) \cdot u(t) \tag{7}$$

where $\Delta f(\mathbf{x}, t)$ represents process uncertainties, unmodeled dynamics, and external disturbances. In this study, we used the earlier canonical form to describe the knee joint dynamics. The module $f(\mathbf{x})$ represents the passive component of knee–joint dynamics utilizing the prior knowledge. The second module $\Delta f(\mathbf{x}, t)$ uses a time-varying neural network to represent the structured and unstructured uncertainties. The third module represents the active dynamics of the muscle. By solving $\dot{s} = 0$ (2) for the control input using (7), we obtain the following expression for equivalent control:

$$u_{\mathrm{eq}}(t) = \frac{1}{\hat{b}(\mathbf{x}, t)} \times \left(-\hat{f}(\mathbf{x}, t) - \Delta\hat{f}(\mathbf{x}, t) + \ddot{x}_d(t) - 2\lambda\dot{e}(t) - \lambda^2 e(t) \right) \cdot \tag{8}$$

The whole control input u_1 applied to the muscle would be combination of u_{eq}(8) and u_c(5).

Modeling Knee Joint Dynamics: To design the controller, the knee joint dynamics is first represented by the following second-order nonlinear equation:

$$\ddot{\theta} = f(\theta, \dot{\theta}) + \Delta f(\theta, \dot{\theta}, t) + b \cdot u(t) \tag{9}$$

where θ and u denote the knee angle and the stimulation intensity, respectively. The nonlinear function $f(\theta, \dot{\theta})$ represents the passive moments acting at the knee as follows:

$$f(\theta, \dot{\theta}) = \frac{1}{J}\left(M_{\mathrm{gra}}(\theta) + M_{\mathrm{ela}}(\theta) + M_{\mathrm{vis}}(\dot{\theta}) \right). \tag{10}$$

Here, $M_{\mathrm{gra}}(\theta)$, $M_{\mathrm{ela}}(\theta)$, and $M_{\mathrm{vis}}(\dot{\theta})$ are gravitational, elastic, and viscous components, respectively. These passive moments were calculated from following equations [30]:

$$M_{\mathrm{gra}}(\theta) = -mgl\,\sin(\theta) \tag{11}$$

$$M_{\mathrm{ela}}(\theta) = -K_1\,\exp(-K_2\theta)(\theta - K_3) \tag{12}$$

$$M_{\mathrm{vis}}(\dot{\theta}) = -B_1\,\mathrm{sgn}(\dot{\theta})\left|\dot{\theta}\right|^{B_2} \tag{13}$$

where l is the distance between knee and center of mass and m is the mass of the shank–foot complex. A pendulum trial without stimulation was performed to identify stiffness and damping parameters. Offline identification of these parameters was performed by a nonlinear least square method. A stochastic pulsewidth stimulation signal in constant amplitude used for calculating the bounds of b and geometric mean of the estimated lower and upper bound of the control gain for estimating b [24]. The parameters were identified during the first experiment and used for subsequent experiments on different days.

Modeling Uncertainties: The nonlinear function $\Delta f(\theta, \dot{\theta}, t)$ represents the system uncertainties including system parameter variations, disturbances, and unmodeled dynamics (e.g., activation dynamics, nonlinear recruitment, muscle fatigue, and multiplicative nonlinear torque–angle and torque–velocity scaling factors). In this study, an RNN with single hidden layer is used to model the system uncertainties. The RNN that involves dynamic elements in the form of feedback loop has a profound impact on the learning capability and performance of the network [31]. Moreover, the feedback loops that feedback the lagged outputs of the neurons to the inputs of neurons, enable the network to perform dynamic mapping and learning tasks that extends over the time. The architecture of the RNN takes many different forms [31]. In this study, we use recurrent multilayer perceptron with single hidden layer, as illustrated in Fig. 1.

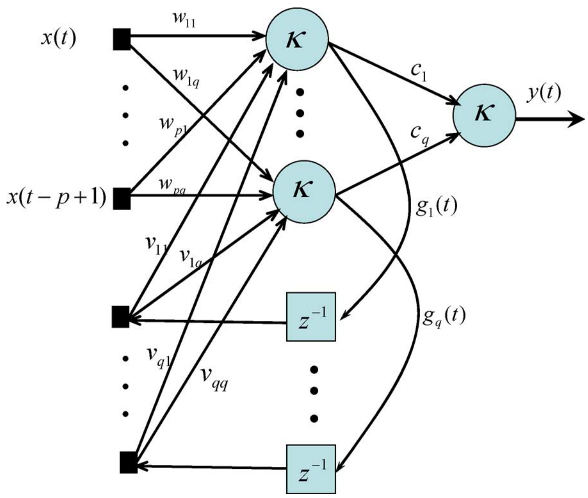

Fig. 1. Structure of the recurrent single-layer neural network.

The network contains recurrent connections from the hidden neurons to a layer consisting of unit delays. The output of unit-delay layer is fed to the input layer. We may then describe the dynamic behavior of the network by the following equations:

$$y(t+1) = \kappa\left(\sum_{i=1}^{q} c_i g_i(t)\right)$$
$$g_i(t) = \kappa\left(\sum_{j=1}^{p} w_{ji}x(t-j+1) + \sum_{k=1}^{q} v_{ki}g_k(t-1)\right) \tag{14}$$

where $\kappa(\cdot)$ is a nonlinear activation function characterizing the hidden and output units, $g_i(t)$ is the response of the ith hidden unit, and c_i is its connecting weight to the output unit. The weight vectors w and v are the connecting weights of the input units and unit-delay units to the hidden units, respectively. The parameters $\Phi = (w, v, c)$ were adjusted by using the standard backpropagation learning algorithm [31]. The cost function J is defined by

$$J(t) = \frac{1}{2}e^2(t) \tag{15}$$

where e is error function defined by

$$e(t) = \ddot{\theta} - \ddot{\theta}_d = \hat{f}(\theta,\dot{\theta}) + \Delta\hat{f}(\theta,\dot{\theta},t) + \hat{b}\cdot u(t) - \ddot{\theta}_d. \tag{16}$$

Considering the gradient descent method, the adaptation rule can be described as follows:

$$\Phi(t+\Delta t) = \Phi(t) - \tau\frac{\partial J(t)}{\partial \Phi(t)} = \Phi(t) - \tau\cdot e(t)\cdot\frac{\partial \Delta\hat{f}(t)}{\partial\Phi(t)} \tag{17}$$

where τ is the learning rate parameter.

B. Neural Control

In order to eliminate high-frequency control and chattering around sliding surface, a single-neuron controller based on the method proposed in [29] is used here. The output of the neuron is given by

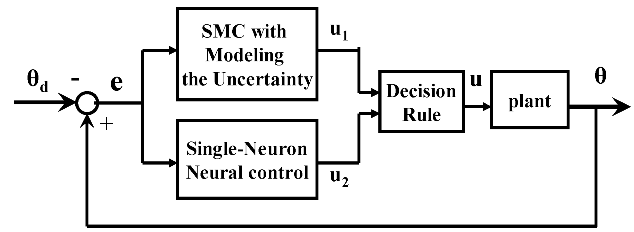

Fig. 2. Neuro-SMC with adaptive modeling of uncertainty.

$$u_2 = h(\mathrm{net}) = \alpha\frac{[1-\exp(-\beta\cdot \mathrm{net})]}{[1+\exp(-\beta\cdot\mathrm{net})]} \tag{18}$$
$$\mathrm{net} = \varepsilon + \dot{\varepsilon} - \gamma \tag{19}$$

where ε is the state error (i.e., $\varepsilon = \theta - \theta_d$), γ is the threshold, and net denotes neuron input. For online adaptation of the network parameters, $\Gamma = [\alpha, \beta, \gamma]^T$, the following Lyapunov function E is defined

$$E = \frac{1}{2}\varepsilon^2.$$

The aim of control is to minimize E by updating the neural controller parameters Γ. It was shown that by using the following adaptation rule [29], the output tracking error asymptotically converges to zero

$$\dot{\Gamma} = -\mu\cdot\varepsilon(t)\cdot\frac{\partial u_2}{\partial\Gamma}\cdot\mathrm{sgn}\left(\frac{\partial\theta}{\partial u}\right) \tag{20}$$

where $\mu > 0$ is the learning rate parameter and $\mathrm{sgn}(\cdot)$ is a sign function.

C. Neuro-SMC

The structure of neural SMC that is based on the combination of neural network and sliding mode is schematically shown in Fig. 2, where u_1 is the SMC output defined in (6) and (8) and u_2 is the neuron output defined in (18). Controller output is a function of u_1 and u_2 defined by

$$u = \begin{cases} u_1, & \text{if } |s(e)| > \phi + \xi \\ \delta(e)u_1 + (1-\delta(e))u_2, & \text{if } \phi < |s(e)| \le \phi + \xi \\ u_2, & \text{if } |s(e)| \le \phi \end{cases} \tag{21}$$

where $s(e)$ is a scalar function described in (2), ϕ and $\xi > 0$ are the boundary layer thicknesses, and $\delta(e)$ is a function of error and is adapted by

$$\delta(e) = \frac{|s(e)| - \phi}{\xi}. \tag{22}$$

IV. Simulation Studies

A model of musculoskeletal presented in [14] was used here as a virtual patient in simulation studies. The model of electrically stimulated muscle used in this study included an input delay, nonlinear recruitment, linear dynamics, and multiplicative nonlinear torque–angle and torque–velocity scaling factors. The skeletal model consisted of a one-segment planar system with passive constraints on joint movement. The set of parameters for muscle and skeletal model are taken from [14].

Parameters of the model (9) that was used for control design were estimated in two steps. At the first step, a passive pendulum trial with no stimulation was performed for identification of passive element (10), $f(\theta, \dot{\theta})$, using nonlinear least square approach. At the second step, a stochastic pulsewidth stimulation signal with constant amplitude was used to determine the bounds of b. The parameters were identified during the first simulation and used for all subsequent evaluations. The RNN used here to represent $\Delta f(\theta, \dot{\theta}, t)$, consisted of ten hidden units and its training was performed online during controlling the joint movement. The root-mean-square (rms) error and normalized rms (nrms) were calculated as a measure of tracking accuracy as follows:

$$\text{rms} = \sqrt{\frac{1}{T}\sum_{t=1}^{T}\left(\theta(t) - \theta_d(t)\right)^2}$$

$$\text{nrms} = \frac{1}{\theta_{\max} - \theta_{\min}}\sqrt{\frac{1}{T}\sum_{t=1}^{T}\left(\theta(t) - \theta_d(t)\right)^2} \times 100.$$

Fig. 3(a) and (b) shows the results of the conventional SMC of the knee joint angle in virtual patient for two different values of boundary layer width. The high control activity and the chattering due to SMC [Fig. 3(a), rms error 4.8° (8%)] are clearly observed. Moreover, increasing the boundary layer thickness reduces chattering but increases the tracking error [Fig. 3(b), rms error 8.9° (14.8%)]. The result of knee joint angle control using neuro-SMC is shown Fig. 3(c) [rms error 2.7° (4.5%)]. It is observed that the chattering of control signals produced by SMC is effectively eliminated even with a thinner boundary layer. It is apparent that the proposed control strategy is able to provide remarkably fast and robust tracking with a smooth control action.

SMC has been known for its capabilities in accounting for modeling imprecision, parameter variations, and bounded disturbances. To assess the versatility of the neuro-SMC controller, the effects of external disturbance, muscle fatigue, and system parameter variations were evaluated as follows.

Effects of External Disturbances: To evaluate the ability of proposed control strategy to external disturbance rejection, a constant torque in amount of 20 Nm (which is about 40% of maximum generated torque during disturbance-free trial) was subtracted suddenly from the torque generated by the muscle for a duration of 50 s. Fig. 4 shows that excellent tracking performance and fast convergence can be achieved under external disturbances using proposed neuro-SMC [rms error 3.3° (5%)].

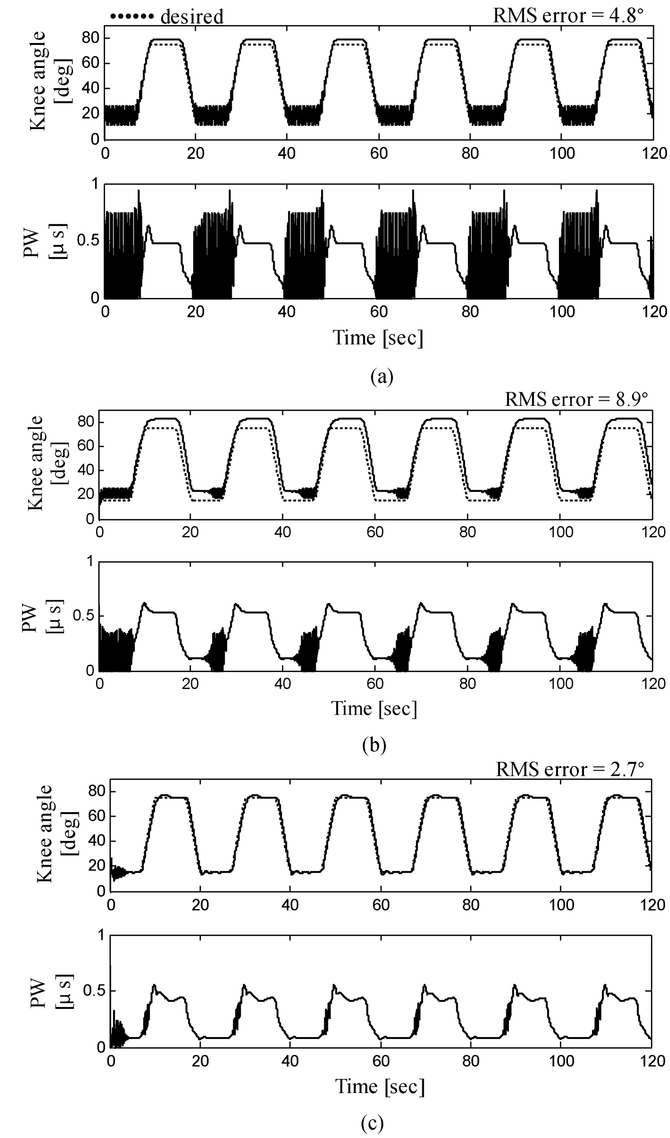

Fig. 3. Simulation results of knee movement control. Conventional SMC ($k = 40, \lambda = 3, \hat{b} = 100$) with boundary layer thicknesses (a) $\phi = 1$ and (b) $\phi = 3$. (c) Neuroadaptive SMC with $k = 40, \lambda = 3, \hat{b} = 100, \xi = 2$, and $\phi = 0.5$.

Effects of Muscle Fatigue: In FNS application, muscle fatigue can cause degradation of system performance. Fatigue was included in the virtual patient to evaluate the capability of the control strategy to compensate for it. As reported in literature, fatigue can cause approximately 50% reduction in peak muscle torque over 100 s [14]. The model of fatigue consisted of an asymptotic decrease in the muscle's input gain to 44% of its original value over 120 s. Fig. 5 demonstrates that the neuro-SMC can also provide a very good tracking performance during muscle fatigue [rms error is 3.7° (6%) over 120 s].

Effects of System Parameter Variations: To evaluate the performance of controller under system parameter variations, several parameters including mass, length, inertia, stiffness, and damping were varied ±50% from their nominal values (The nominal values were 10 kg, 0.4 m, 0.1 kg·m^2, 20 N·m/°, and 1 N·m/(°·s), respectively.) The model of the virtual patient was identified during first simulation with nominal values of system

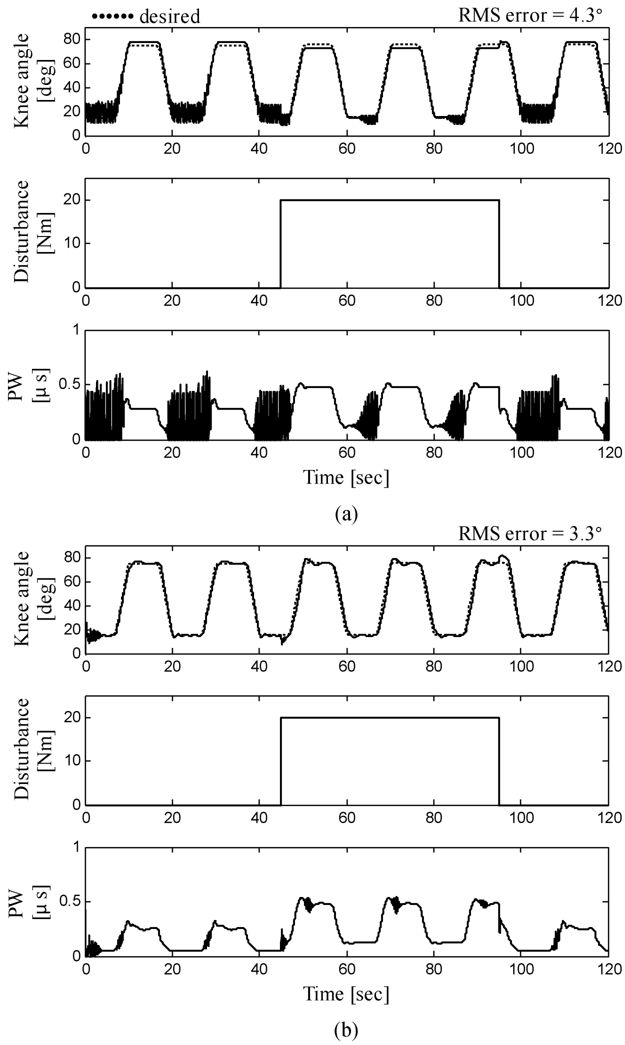

Fig. 4. Simulation results of external disturbance rejection obtained using (a) conventional SMC ($k = 40, \lambda = 3, \hat{b} = 100, \phi = 1$) and (b) neuroadaptive SMC ($k = 40, \lambda = 3, \hat{b} = 100, \xi = 2, \phi = 0.5$).

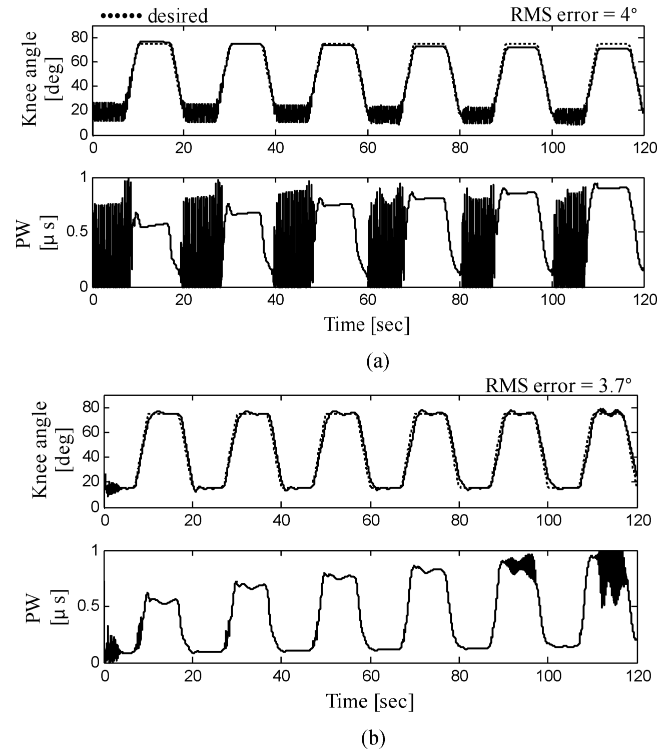

Fig. 5. Simulation results of fatigue compensation obtained using (a) conventional SMC ($k = 40, \lambda = 3, \hat{b} = 100, \phi = 1$) and (b) neuroadaptive SMC ($k = 40, \lambda = 3, \hat{b} = 100, \xi = 2, \phi = 0.5$).

parameters. Table I summarizes the average tracking error over a wide range of system parameters using the model identified during first simulation with nominal values of system parameters. For the worst trial, tracking error is less than 14.0% (8.2°) and 7.0% (3.9°) using traditional SMC and proposed neuro-SMC, respectively. This interesting result indicates that the proposed control strategy can be used for different subjects without any re-identification of the plant model and can compensate the time-varying properties of neuromuscular dynamics.

V. Experimental Evaluation

A. Experimental Procedure

Experiments were conducted on five complete thoracic paraplegic (Table II) and four healthy subjects using an eight-channel computer-based closed-loop FNS system [32]. Each subject participated in three experiment sessions. Each session was conducted on a different day and consisted of at least five trials with intertrial resting interval at least 5 min. Duration of each trial is 120 s for normal test and 180 s for fatigue test. The paraplegic subjects were active participants in a rehabilitation research program involving daily electrically stimulated exercise of their lower limbs (either seated or during standing and walking). The subject was seated on a bench with his hip flexed at approximately 90°, while the shank was allowed to swing freely. The quadriceps muscle was stimulated using adhesive surface elliptical electrodes (5×10 cm GymnaUniphy electrodes, COMEPA Industries, Belgium) that were placed just proximally over the estimated motor point of rectus femoris and the approximately 4-cm proximal of the patella. Pulsewidth modulation (from 0 to 700 μs) with balanced bipolar stimulation pulses, at a constant frequency (25 Hz) and constant amplitude was used. An electrogoniometer (model SG150, Biometrics Ltd., Gwent, U.K.) is fixed on the knee joint to measure the knee joint position. The measured signals were sampled at 1 kHz by a 12-bit analog-to-digital converter (Advantech PCI-1711 I/O card).

The computer-based closed-loop FNS system uses MATLAB Simulink (The Mathworks, 1998–2000), Real-Time Workshop, and Real-Time Windows Target under Windows 2000/XP for online data acquisition, processing, and controlling. The proposed control strategy was implemented by S-functions using C.

Two different types of desired movement trajectories were used to evaluate the stability and tracking performance of the proposed strategy. The first one was a ramp-hold-ramp trajectory corresponding to real walking trajectory movement with a period of 20 s and a duty cycle of 70% [14 s on (movement

TABLE I
SUMMARY OF RMS ERROR OBTAINED DURING SYSTEM PARAMETER VARIATIONS USING TRADITIONAL SMC AND PROPOSED NEUROADAPTIVE SMC

Controller	Mass (kg)	Length (m)	Inertia (kgm^2)	Stiffness (Nm/ °)	Damping (Nm/ °/sec)
	10 ± 5	0.4 ± 0.2	0.1 ± 0.05	20 ± 10	1 ± 0.5
Conventional SMC	< 6.5°	< 5.9°	< 5.1°	< 8.2°	< 5.2°
Neuro-Adaptive SMC	< 3.6°	< 3.7°	< 2.7°	< 3.9°	< 2.7°

The parameters were varied ±50% from their nominal values.

TABLE II
CLINICAL CHARACTERISTICS OF NEUROPROSTHESIS RECIPIENTS

Subject	Level of SCI	Date of Injury	FNS Training
HA	T9-T10	2002	4 Months
MH	T5-T6	2000	1 Year
RO	T6	1999	2 Months
RR	T7	1997	4 Years
MS	T10-T11	2001	2 Years

phase) and 6 s OFF (rest phase)]. The second one was a raised cosine with a period of 12 s and a duty cycle of 50% [6 s ON (movement phase) and 6 s OFF (rest phase)]. The range of motion is between 18° and 78°.

B. Experimental Results

The identification of knee joint dynamics was conducted in the same way as the simulation study. First, a passive pendulum trial with no stimulation was performed for identification of passive element (13), $\hat{f}(\theta, \dot{\theta})$, using nonlinear least square approach. Next, a stochastic pulsewidth stimulation signal with constant amplitude was used to determine the parameter b. The $\hat{f}(\theta, \dot{\theta})$ and $\hat{b}$ were identified during first session of experiment on one subject. The values of identified parameters were used for subsequent experiment sessions on different days for all subjects. The adaptation of RNN was performed during online control without any offline training.

Examples of joint angle trajectories obtained with traditional SMC and neuro-SMC on a healthy subject are shown in Fig. 6. The chattering effect of conventional SMC that is caused by high-speed switching control can be clearly observed [Fig. 6(a), rms error 5.49° (9%)]. Although increasing the boundary layer thickness can reduce the chattering effects, but it causes the tracking error to be increased [Fig. 6(b), rms error 6.67° (11%)]. Excellent tracking performance with no chattering is achieved using proposed neuro-SMC [Fig. 6(c) rms error 2.56° (4%)]. An interesting observation is the fast convergence of proposed method. The actual joint angle converges to its desired trajectory within about 2 s.

Fig. 7 shows the same information as in Fig. 6 when the experiments were conducted on paraplegic subject RR. Although the boundary layer approach was used to eliminate the chattering, the effects of high switching activity are noticeable [Fig. 7(a)]. It is observed that the control signal increases and reaches its maximum value, while the joint angle could not track the desired trajectory [Fig. 7(a)]. This observation indicates the early induction of muscle fatigue. In contrast, an accurate tracking of desired motion with no chattering was obtained using proposed neuro-SMC on paraplegic subject RR [Fig. 7(b), rms error 3.54° (6%)]. The results obtained from Figs. 6 and 7 clearly indicate the superior performance of proposed method with respect to classical SMC. Fig. 8 shows typical tracking results obtained

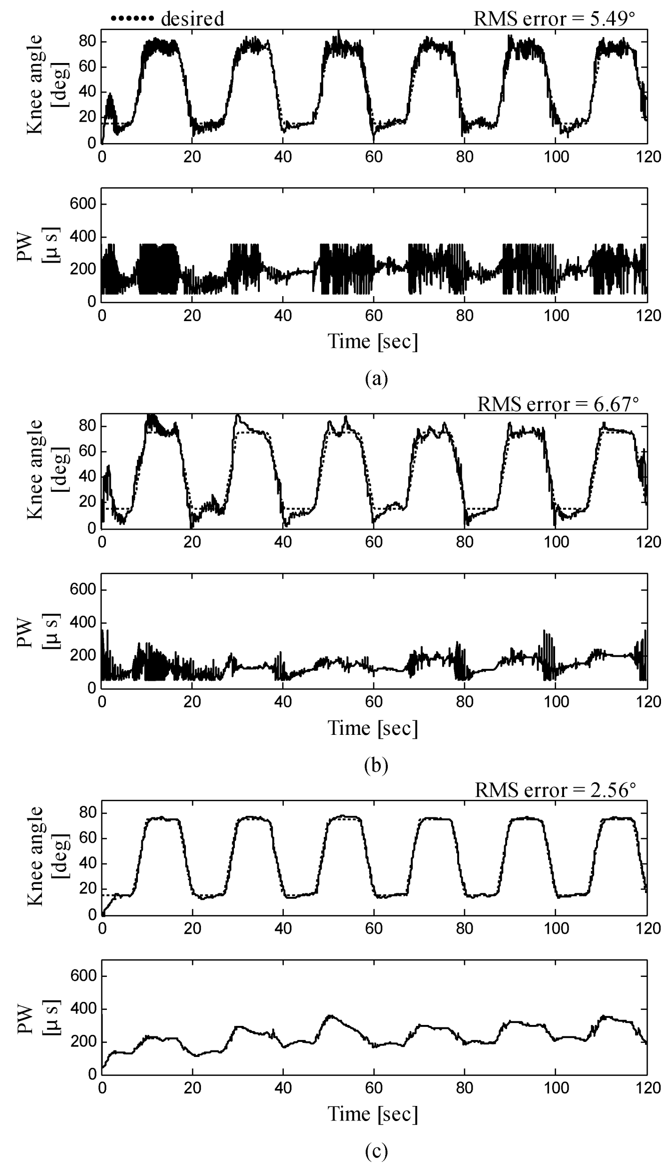

Fig. 6. Results of the knee movement control on healthy subject AA. Conventional SMC $(k = 40, \lambda = 3,\ \hat{b} = 72)$ with boundary layer thicknesses (a) $\phi = 20$ and (b) $\phi = 30$. (c) Neuroadaptive SMC with $k = 35, \lambda = 3, \hat{b} = 72, \xi = 10$, and $\phi = 2$.

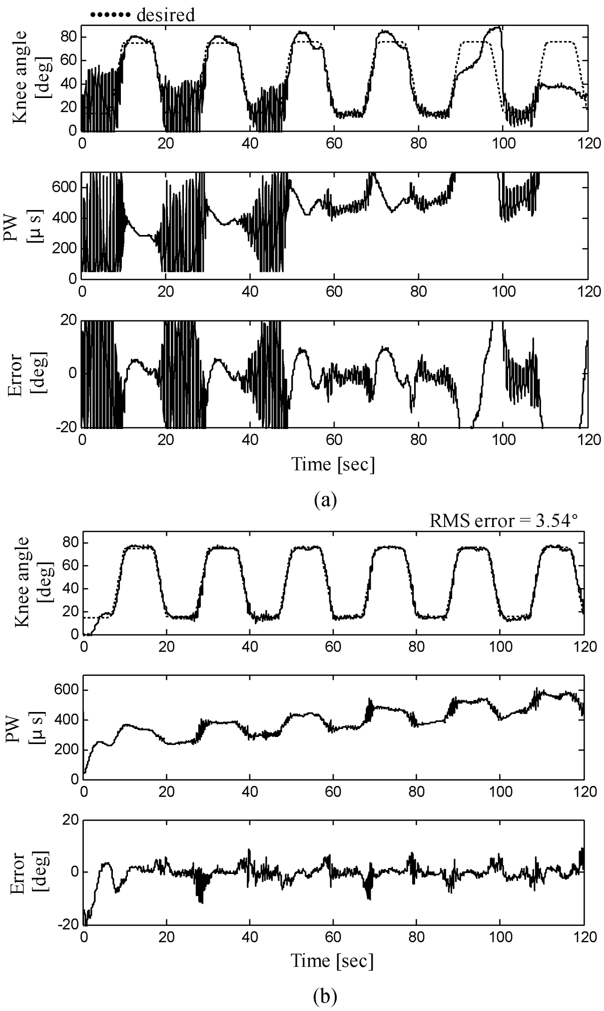

Fig. 7. Results of the knee movement control on paraplegic subject RR using (a) conventional SMC ($k = 40, \lambda = 3, \phi = 30, \hat{b} = 72$) and (b) neuroadaptive SMC ($k = 35, \lambda = 3, \hat{b} = 72, \xi = 10, \phi = 2$).

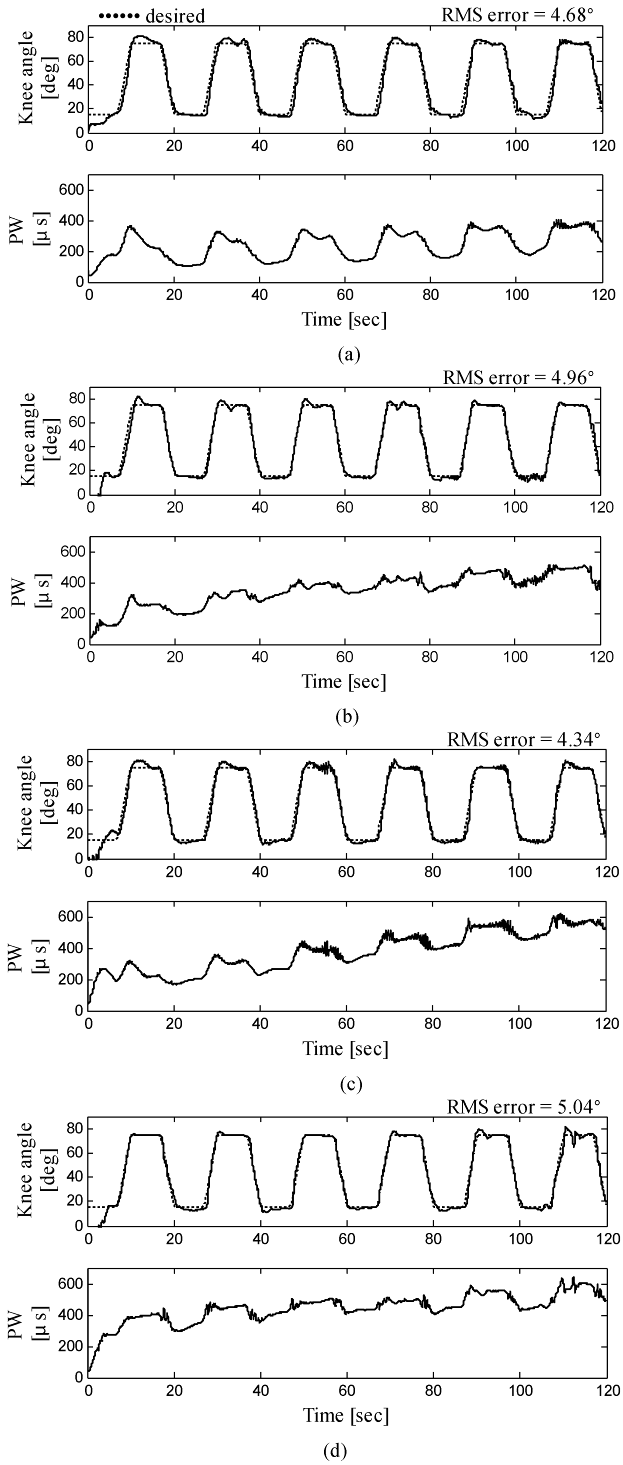

Fig. 8. Typical tracking results obtained using neuroadaptive SMC ($k = 35, \lambda = 3, \hat{b} = 72, \xi = 10, \phi = 2$) for paraplegic subjects (a) HA, (b) RO, (c) MH, and (d) MS.

using neuro-SMC with adaptive modeling of uncertainty for other paraplegic subjects. The most interesting observation is the fast convergence of the proposed control strategy. The knee movement trajectory converges to the desired trajectory after about 3 s. The same results were obtained in all experiment trials that were conducted on healthy and paraplegic subjects during different days. A summary of results over 135 trials on healthy and paraplegic subjects (see Table III) indicates that the proposed control strategy was able to achieve a good tracking performance by adapting the stimulation pattern. Average rms tracking error is $3.76^\circ \pm 0.25^\circ$ for a 60° range of movement for able-bodied, while it is $5.41^\circ \pm 0.26^\circ$ for paraplegic subjects.

Muscle Fatigue Compensation: Fig. 9 shows the ability of neuro-SMC to compensate the muscle fatigue for a raised cosine trajectory. The average of rms error is about 3.7° (6.2%) for a 60° range of movement over 3 min. The results show that the method could adjust the stimulation pattern to compensate the muscle fatigue. It is observed that the joint angle trajectory converges to the desired trajectory after about 2 s and tracking performance remains fairly constant throughout the trial. It should be noted that the values of model parameters (14)–(16) were set to the same values that were determined during the first day experiment on one subject and the learning of neural networks performed online without any offline training.

Effects of External Disturbances: Fig. 10 shows the result of external disturbance rejection using neuro-SMC. The disturbance was realized by gently applying a load (1.5 kg) on the ankle at $t = 33$ s and removing it at $t = 73$ s. It is observed that

TABLE III
SUMMARY OF AVERAGE DAILY RMS TRACKING ERROR (±1 STANDARD DEVIATION) OBTAINED USING PROPOSED NEUROADAPTIVE SMC [(a) HEALTHY SUBJECTS AND (b) PARAPLEGIC SUBJECTS]

(a)

Subject	Day1	Day2	Day3
AA	$2.95^\circ \pm 0.35^\circ$	$3.17^\circ \pm 0.32^\circ$	$2.90^\circ \pm 0.37^\circ$
ME	$3.72^\circ \pm 0.47^\circ$	$3.08^\circ \pm 0.14^\circ$	$2.85^\circ \pm 0.27^\circ$
KM	$4.72^\circ \pm 0.15^\circ$	$4.78^\circ \pm 0.13^\circ$	$3.61^\circ \pm 0.19^\circ$
HK	$4.39^\circ \pm 0.29^\circ$	$4.45^\circ \pm 0.15^\circ$	$4.52^\circ \pm 0.21^\circ$
Mean	$3.76^\circ \pm 0.25^\circ$		

(b)

Subject	Day1	Day2	Day3
RR	$5.59^\circ \pm 0.19^\circ$	$5.34^\circ \pm 0.10^\circ$	$4.45^\circ \pm 0.23^\circ$
MH	$6.40^\circ \pm 0.17^\circ$	$4.92^\circ \pm 0.15^\circ$	$4.69^\circ \pm 0.28^\circ$
HA	$5.94^\circ \pm 0.30^\circ$	$5.44^\circ \pm 0.23^\circ$	$4.81^\circ \pm 0.32^\circ$
RO	$5.85^\circ \pm 0.33^\circ$	$5.34^\circ \pm 0.55^\circ$	$5.37^\circ \pm 0.17^\circ$
MS	$6.01^\circ \pm 0.23^\circ$	$5.03^\circ \pm 0.30^\circ$	$6.04^\circ \pm 0.31^\circ$
Mean	$5.41^\circ \pm 0.26^\circ$		

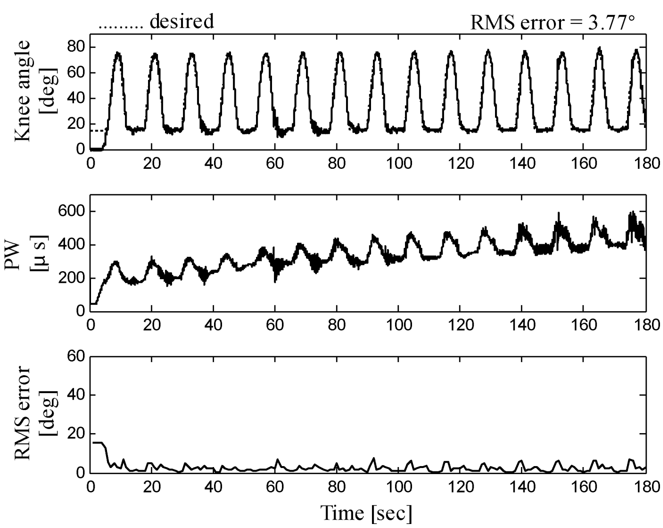

Fig. 9. Ability of proposed neuroadaptive SMC to compensate the muscle fatigue for a raised cosine desired movement trajectory.

a perfect disturbance rejection is obtained through the proposed SMC [rms error 4.72° (7.8%)]. The interesting observation is the fast convergence of tracking trajectory at the time of applying the disturbance.

VI. DISCUSSION AND CONCLUSION

In this paper, a novel control strategy incorporating the SMC, neural network, and adaptive control has been proposed for controlling the FES. Simulation studies on a virtual patient demonstrated the exceptional performance and robustness of the proposed control system against system parameter variations, muscle fatigue, external disturbances, and unmodeled dynamics. Extensive experiments on healthy and paraplegic subjects confirm the results obtained by simulation studies.

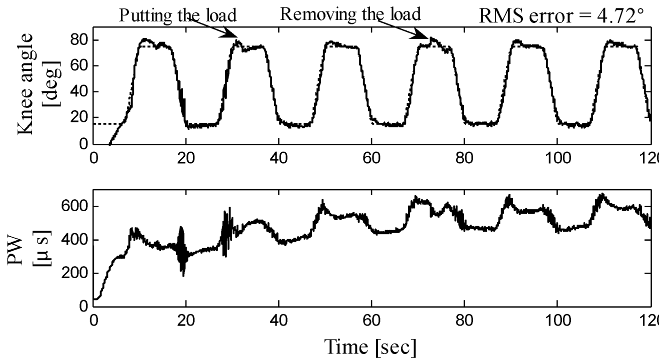

Fig. 10. Effect of external disturbance rejection using proposed neuro-SMC in paraplegic subject MH. A load (1.5 kg) was applied on the ankle at $t = 33$ s and removed at $t = 73$ s.

An important result observed is the fast convergence of the control system. The knee movement trajectory converges to the desired trajectory after about 2 s. This observation is the direct consequence of the exponential convergence rate of tracking error in SMC. In contrast, adaptive control is able to achieve only asymptotic convergence. Riess and Abbas [16] who used an adaptive feedforward controller for controlling the knee joint angle to track a raised cosine trajectory, reported that the tracking error for the first few cycle was very large and reduced to within 10% after an average of 30 cycles (75 s). In [13], the results of two experimental trials on two paraplegic subjects using an adaptive feedforward controller showed that controller took more than 20 s to converge.

The most current adaptive controllers for FES applications required pretraining and offline identification before they could be used to control the limbs (e.g., see [12], [13], and [19]). Ferrarin *et al.* [13] used a Hill-based model of knee joint dynamics to develop an adaptive feedforward controller. The model was identified in several separate experiments [33], [34] that makes the parameter identification to be complex. Kurosawa *et al.* [19] who used an adaptive feedforward neural controller for controlling the palmar/dorsi-flexion angle of the wrist, reported that the untrained controller is almost identical to the PID controller and learning iteration was shortened if the feedforward controller had been trained in advance with the artificial forward model. The burdens of pretraining may hinder the clinical applications of these methods.

A major contribution of our work in this study is that the proposed control scheme does not require re-identification of the plant model during different experiment sessions, different experiment days, and even for applying the controller on the new subjects. Two neural networks that were coupled into the SMC were trained online during applying the controller on paralyzed limb without any pretraining or offline training. The knee movement trajectory will converge to the desired trajectory after about 2 s. This observation has great implications for clinical applications and is the results of robustness of SMC to model uncertainties.

The results presented here have been verified only for control of movement in a single joint. The extension of the study to control of cyclic movement, standing up, sitting down, and free support standing using the proposed control strategy constitutes the key issues of our current research.

References

[1] D. Graupe, R. Davis, H. Kordylewski, and K. Kohn, "Ambulation by traumatic T4-T12 paraplegics using functional neuromuscular stimulation," *Crit. Rev. Neurosurg.*, vol. 8, no. 4, pp. 221–231, Jul. 1998.

[2] D. Popovic and T. Sinkjaer, *Control of Movement for the Physically Disabled*. New York: Springer-Verlag, 2000.

[3] M. R. Popovic, T. Keller, I. P. I. Pappas, V. Dietz, and M. Morari, "Surface-stimulation technology for grasping and walking neuroprostheses," *IEEE Eng. Med. Biol. Mag.*, vol. 20, no. 1, pp. 82–93, Jan. 2001.

[4] G. M. Lyons, T. Sinkær, J. H. Burridge, and D. J. Wilcox, "A review of portable FES-based neural orthoses for the correction of drop foot," *IEEE Trans. Neural Syst. Rehabil. Eng.*, vol. 10, no. 4, pp. 260–279, Dec. 2002.

[5] S. Agarwal, R. J. Triolo, and R. Kobetic, "Long-term user perceptions of an implanted neuroprosthesis for exercise, standing, and transfers after spinal cord injury," *J. Rehabil. Res. Dev.*, vol. 40, no. 3, pp. 241–252, May/Jun. 2003.

[6] J. J. Abbas and H. J. Chizeck, "Feedback control of coronal plane hip angle in paraplegic subjects using functional neuromuscular stimulation," *IEEE Trans. Biomed. Eng.*, vol. 38, no. 7, pp. 687–698, Jul. 1991.

[7] N. Lan, P. E. Crago, and H. J. Chizeck, "Control of end-point forces of multi-joint limb by functional electrical stimulation," *IEEE Trans. Biomed. Eng.*, vol. 38, no. 10, pp. 935–965, Oct. 1991.

[8] L. A. Bernotas, P. E. Crago, and H. J. Chizeck, "Adaptive control of electrically stimulated muscle," *IEEE Trans. Biomed. Eng.*, vol. 34, no. 2, pp. 140–147, Feb. 1987.

[9] M. S. Hawell, B. J. Oderkek, C. A. Sacher, and G. F. Inbar, "The development of a model reference adaptive controller to control the knee joint of paraplegics," *IEEE Trans. Automat. Contr.*, vol. 36, no. 6, pp. 683–691, Jun. 1991.

[10] J. J. Abbas and H. J. Chizeck, "Feedback control methods for task regulation by electrical stimulation of muscle," *IEEE Trans. Biomed. Eng.*, vol. 38, no. 12, pp. 1213–1223, Dec. 1991.

[11] F. Previdi and E. Carpanzano, "Design of a gain scheduling controller for knee-joint angle control by using functional electrical stimulation," *IEEE Trans. Contr. Syst. Technol.*, vol. 11, no. 3, pp. 310–324, May 2003.

[12] G. C. Chang, J. J. Luh, G. D. Liao, J. S. Lai, C. K. Cheng, B. L. Kuo, and T. S. Kuo, "A neuro-control system for the knee joint position control with quadriceps stimulation," *IEEE Trans. Rehabil. Eng.*, vol. 5, no. 1, pp. 2–11, Mar. 1997.

[13] M. Ferrarin, F. Palazzo, and R. Riener, "Model based control of FES-induced single joint movements," *IEEE Trans. Neural Syst. Rehabil. Eng.*, vol. 9, no. 3, pp. 245–257, Sep. 2001.

[14] J. J. Abbas and H. J. Chizeck, "Neural network control of functional neuromuscular stimulation systems: computer simulation studies," *IEEE Trans. Biomed. Eng.*, vol. 42, no. 11, pp. 1117–1127, Nov. 1995.

[15] J. J. Abbas and R. J. Triolo, "Experimental evaluation of an adaptive feedforward controller for use in functional neuromuscular stimulation systems," *IEEE Trans. Rehabil. Eng.*, vol. 5, no. 1, pp. 12–22, Mar. 1997.

[16] J. Riess and J. J. Abbas, "Adaptive neural control of cyclic movements using functional neuromuscular stimulation," *IEEE Trans. Rehabil. Eng.*, vol. 8, no. 1, pp. 42–52, Mar. 2000.

[17] J. Reiss and J. Abbas, "Adaptive control of cyclic movements as muscles fatigue using functional neuromuscular stimulation," *IEEE Trans. Neural Syst. Rehabil. Eng.*, vol. 9, no. 3, pp. 326–330, Sep. 2001.

[18] A. R. Mirizarandi, A. Erfanian, and H. R. Kobravi, "Adaptive inverse control of knee joint position in paraplegic subjects using recurrent neural network," presented at the 10th Annu. Conf. Int. Functional Electr. Stimul. Soc., Montreal, QC, Canada, 2005.

[19] K. Kurosawa, R. Futami, T. Watanabe, and N. Hoshimiya, "Joint angle control by FES using a feedback error learning controller," *IEEE Trans. Neural Syst. Rehabil. Eng.*, vol. 13, no. 3, pp. 359–371, Sep. 2005.

[20] P. A. Ioannou and J. Sun, *Robust Adaptive Control*. Englewood Cliffs, NJ: PTR Prentice-Hall, 1996.

[21] D. Hongliu and S. S. Nair, "Learning control design for a class of nonlinear systems," *Eng. Appl. Artif. Intell.*, vol. 11, no. 4, pp. 495–505, Aug. 1998.

[22] T. Zhang, S. S. Ge, C. C. Hang, and T. Y. Chai, "Adaptive control of first-order systems with nonlinear parameterization," *IEEE Trans. Automat. Contr.*, vol. 45, no. 8, pp. 1512–1516, Aug. 2000.

[23] D. E. Miller, "A new approach to model reference adaptive control," *IEEE Trans. Automat. Contr.*, vol. 48, no. 5, pp. 743–757, 2003.

[24] J. J. E. Slotine and W. Li, *Applied Nonlinear Control*. Englewood Cliffs, NJ: Prentice-Hall, 1991.

[25] K. D. Young, V. Utkin, and U. Ozguner, "A control engineer's guide to sliding mode control," *IEEE Trans. Control Syst. Technol.*, vol. 7, no. 3, pp. 328–342, May 1999.

[26] J. Guldner and V. Utkin, "The chattering problem in sliding mode systems," presented at the 14th Int. Symp. Math. Theory Netw. Syst. (MTNS), Perpignan, France, 2000.

[27] T. Schauer, W. Holderbaum, and K. J. Hunt, "Sliding-mode control of knee-joint angle: experimental results," presented at the 7th Annu. Conf. Int. Functional Electr. Stimul. Soc., Ljubljana, Slovenia, 2002.

[28] S. Jezernik, R. G. V. Wassink, and T. Keller, "Sliding mode closed-loop control of FES: controlling the shank movement," *IEEE Trans. Biomed. Eng.*, vol. 51, no. 2, pp. 263–272, Feb. 2004.

[29] W. D. Chang, R. C. Hwang, and J. G. Hsieh, "Application of an auto-tuning neuron to sliding mode control," *IEEE Trans. Syst., Man, Cybern. C, Appl. Rev.*, vol. 32, no. 4, pp. 517–522, Nov. 2002.

[30] T. Schauer, N.-O. Negård, F. Previdi, K. J. Hunt, M. H. Fraser, E. Ferchland, and J. Raisch, "Online identification and nonlinear control of the electrically stimulated quadriceps muscle," *Control Eng. Practice*, vol. 13, no. 9, pp. 1207–1219, 2005.

[31] A. C. Tsoi and A. D. Back, "Locally recurrent globally feedforward networks: A critical review of architectures," *IEEE Trans. Neural Netw.*, vol. 5, no. 2, pp. 229–239, Mar. 1994.

[32] H. R. Kobravi and A. Erfanian, "A transcutaneous computer-based closed-loop motor neuroprosthesis for real-time movement control," presented at the 9th Annu. Conf. Int. Functional Electr. Stimul. Soc., Bournemouth, U.K., 2004.

[33] R. Riener and T. Edrich, "Identification of passive elastic joint moments in the lower extremities," *J. Biomech.*, vol. 32, no. 5, pp. 539–544, May 1999.

[34] T. Edrich, R. Riener, and J. Quintern, "Analysis of passive elastic joint moments of the lower extremities in paraplegics and normal controls," *IEEE Trans. Biomed. Eng.*, vol. 47, no. 8, pp. 1058–1065, Aug. 2000.

Arash Ajoudani received the B.Sc. degree in biomedical engineering from Amirkabir University of Technology (Polytechnic), Tehran, Iran, in 2004, and the M.Sc. degree in biomedical engineering from Iran University of Science and Technology (IUST), Tehran, in 2007.

Since 2004, he has been with FES research group in Neuromuscular Control Systems Laboratory, IUST. His current research interests include functional electrical stimulation in paraplegic subjects and robust and adaptive control.

Abbas Erfanian (M'09) received the B.Sc. degree in computer engineering from Shiraz University, Shiraz, Iran, in 1985, the M.Sc. degree in computer engineering from Sharif University of Technology, Tehran, Iran, in 1989, the Ph.D. degree in biomedical engineering from Tarbiat Modarres University, Tehran, in 1995.

From 1993 to 1994, he was a Senior Research Associate at Case Western Reserve University and VA Medical Center, Cleveland, OH, where he was engaged in the research of functional electrical stimulation and neuromuscular control systems. Since 1995, he has been a faculty member at Iran University of Science and Technology (IUST), Tehran, Iran, where he was the Head of the Department of Biomedical Engineering from 2000 to 2008, and is currently an Associate Professor of biomedical engineering and the Director of Neuromuscular Control Systems Laboratory and Brain–Computer Interface Laboratory, Iran Neural Technology Research Center, IUST. His current research interests include artificial neural network, biomedical signal processing, chaos theory and its application to biomedical problems, brain–computer interface, and functional neuromuscular stimulation. The principal focus of his research is on the control of functional electrical stimulation and its application in spinal cord injury subjects.

Dr. Erfanian is a member of International Functional Electrical Stimulation Society (IFESS).